DOI: 10.1002/cphc.200700339

Dipole Moment Enhancement in Molecular Crystals from X-ray Diffraction Data

Mark A. Spackman,* Parthapratim Munshi, and Birger Dittrich[a]

Although reliable determination of the molecular dipole moment from experimental charge density analyses on molecular crystals is a challenging undertaking, these values are becoming increasingly common experimental results. We collate all known experimental determinations and use this database to identify broad trends in the dipole moment enhancements implied by these measurements as well as outliers for which enhancements are pronounced. Compelling evidence emerges that molecular dipole moments from X-ray diffraction data can provide a wealth of information on the change in the molecular charge distribution that results from crystal formation. Most importantly, these experiments are unrivalled in their potential to provide this information in such detail and deserve to be exploited to a much greater extent. The considerable number of experimental determinations now available has enabled us to pinpoint those studies that merit further attention, either because they point unequivocally to a considerable enhancement in the crystal (of 50% or more), or because the experimental determinations suggest enhancements of 100% or more—much larger than independent theoretical estimates. In both cases further detailed experimental and theoretical studies are indicated.

1. Introduction

Molecular properties have long been used to help rationalize intermolecular interactions, and they are key determinants of bulk properties of the liquid or crystal. However, bulk properties cannot be obtained by simple summation of the properties of isolated molecules, and for this reason information about the properties of molecules in crystals can provide valuable insight into the ways in which these properties are modified by various intermolecular interactions upon incorporation of single molecules into the bulk. One of the simplest such properties, the dipole moment of a molecule in a crystal, is now a common outcome of a quantitative charge density analysis of accurate single crystal X-ray diffraction data, and these experiments are unique in their potential to provide detailed information of this kind.

In their recent review of chemical information accessible from X-ray charge density analyses, Koritsanszky and Coppens comment that "the evidence overwhelmingly points to an often pronounced, crystal-packing dependent, enhancement of the dipole moments of molecules in crystals."[1] A striking example of such a pronounced enhancement was reported some time ago for 2-methyl-4-nitroaniline (MNA), where the X-ray-derived dipole moment was determined to be 25(8) D, considerably greater than the theoretical value of 8.8 D for an isolated molecule,[2] and suggesting an enhancement of $\approx$200%. That work has been highly cited as a prime example of the potentially very large effect of intermolecular interactions and of the crystal field on the electric properties of molecules in suitable crystalline environments. However, a careful and detailed reassessment of this result, based on new X-ray and neutron diffraction data at 100 K, has recently concluded that the molecular dipole moment in the crystal is closer to 12.4(13) D,[3] which represents a considerable enhancement, but far less than previously reported. Since the earlier report of a pronounced dipole moment enhancement for MNA has been followed by a number of similar reports on other molecular crystals, the revised result for MNA has led us to question all reported examples of enhancements of molecular dipole moments based on multipole refinement of X-ray diffraction data, especially where the enhancement exceeds 100%.

We report a critical and comprehensive review of molecular dipole moments derived from X-ray diffraction charge density studies published to date (early 2007). The majority (85%) of these determinations have been published since the first review of this subject by one of us in 1992,[4] and the available data now comprises some 129 determinations based on 70 published studies. Together, these offer the possibility, for the first time, of extracting meaningful trends and identifying outliers, with a view to establishing which are physically meaningful and which are not. For the latter, we hope to identify more precisely the reasons why they are likely to be in error. For a selection of compounds, we also compare the experimental results with those from partitioning of ab initio periodic Hartree–Fock (PHF) electron densities, as well as results based on the use of Lorentz factor tensors to estimate the electric field arising from surrounding molecules and its effect on the molecular dipole moment.[5] Further insight for all systems could undoubtedly come from a consideration of the change in direction as well as the change in magnitude of the dipole moment

[a] *Prof. M. A. Spackman, Dr. P. Munshi, Dr. B. Dittrich*
School of Biomedical, Biomolecular & Chemical Sciences
University of Western Australia
Crawley WA 6009 (Australia)
Fax: (+61) 8-6488-1005
E-mail: mas@cyllene.uwa.edu.au

vector. However, although individual vector components are always computed in charge density studies, they are not usually published. We concentrate solely on the magnitude of the dipole moment vector (referring to it rather loosely as the dipole moment), and leave more detailed investigations for the future. Although we focus on dipole moments obtained from X-ray diffraction data and from theory, we note that there are a number of other experimental techniques commonly used to determine molecular dipole moments, which are based on measurements of either the dielectric permittivity of gases, solutions, or pure liquids, or on the application of the Stark effect to microwave spectroscopy of gases, and we refer the reader to the earlier review[4] for a more detailed discussion of those techniques.

2. Dipole Moments from Experiment and Theory

2.1 Multipole Modeling of Single Crystal X-ray Diffraction Data

The derivation of molecular dipole moments from X-ray diffraction data relies on multipole pseudoatom modeling of the experimental structure factors to deconvolute the electron distribution from the motion of the nuclei, resulting in an analytical representation of the static electron density in the crystal.[6–9] There has been considerable discussion in the literature regarding the problems and uncertainties inherent to determining dipole moments for molecules from multipole refinement of X-ray diffraction data, and the main points can be summarized as follows:[1,4,10,11]

1) The modeling process yields a periodic electron distribution for the crystal, hence extraction of a molecular moment requires a definition of a molecule in a crystal, that is, an arbitrary partitioning of the crystal electron density into molecular fragments.
2) Inherent limitations of the multipole model itself, such as the choice and flexibility of radial functions, their radial extent, the level of the multipole expansion at each atomic site, and the modeling of atomic nuclear motion, can all significantly affect the outcome.
3) As the modeling process involves a least-squares fit to experimental structure factor magnitudes (or their squares), successful treatment of systematic effects in the diffraction measurements (e.g. extinction) is essential.
4) Special difficulties may be encountered in least-squares fits to data for compounds crystallizing in non-centrosymmetric (acentric) space groups, where the phases of the structure factors are also unknown.
5) Error estimates in molecular dipole moments are origin-dependent unless the modelling process incorporates an electroneutrality constraint for the molecule.[12]

2.2 Partitioning the Crystal Electron Density

The problem of partitioning a crystal electron density into identifiable molecules applies equally well to both experimental and theoretical estimates of a molecular dipole moment in the bulk. For experimental electron densities based on the multipole model, a natural partitioning is obtained by summing all multipole functions on all atoms belonging to the molecule in question, thereby obtaining molecular fragments whose electron densities overlap with one another. This is by far the most common way of obtaining a molecular dipole moment from X-ray diffraction data, and it forms the basis of all the results presented in Tables 1 and 2. Alternative methods involve partitioning the crystal electron density into discrete nonoverlapping atomic or molecular fragments. The most common method is based on Bader's quantum theory of atoms in molecules (QTAM),[13] using the topology of the crystal electron density to define atomic basins, from which atomic electron densities, atomic charges, and dipole moments are obtained. These can, in turn, be used to compute a molecular dipole moment. This approach has a firm basis in quantum mechanics and is the method of choice in theoretical calculations. It is also being applied increasingly to experimental model electron densities obtained from a multipole refinement process. It does have limitations, as it requires highly accurate three-dimensional numerical integrations over all atomic basins comprising the molecule, and hence for large molecules can be time-consuming. It should also not be forgotten that the experimental electron density is not a quantum object[14] and does not satisfy basic quantum-mechanical criteria (e.g. it is not necessarily positive everywhere in the unit cell). An alternative discrete partitioning method based on Hirshfeld's sharing function[15] defines a smooth boundary for a molecule in a crystal,[16] and we have recently shown that these molecular Hirshfeld surfaces can be exploited to obtain molecular dipole moments via two-dimensional integration of the electrostatic potential and electric field on the surface.[17] This approach also has a drawback, as it is not an exhaustive partitioning. Hence, small voids remain, which typically contain $\approx 0.1\,\%$ of the electron count of a molecule. Nevertheless, we make use of both QTAM and Hirshfeld surface approaches in the following sections to benchmark some of the results obtained from multipole refinement methods.

2.3 Enhancement of the Dipole Moment

Calculation of the enhancement of a dipole moment begs an obvious question: what to use as a reference value. In the process of crystal formation, both the molecule's geometry and charge density are deformed, which involves a cost in energy that must be more than compensated by a gain in lattice energy. There is therefore considerable choice of reference state:

1) a theoretical calculation on an isolated gas-phase molecule, using either the crystal geometry or an optimized geometry;

Table 1. Full details of space groups, HF/6-31G(d,p) dipole moments, X-ray-derived dipole moments and enhancements, and references to relevant charge density studies, for data in Figures 1 and 2.

Formula	Refcode	Compound name	Space group	$\mu_{6\text{-}31G(d,p)}$	$\mu_{X\text{-}ray}$	$\%\Delta\mu_{X\text{-}ray}$
H_2O	OXACDH06	oxalic acid dihydrate	$P2_1/n$	2.20	2.1(2)[44]	−5(9)
H_2O	CYTOSM03, CYTOSM12	cytosine monohydrate	$P2_1/c$	2.22, 2.24	2.3(3),[45] 3.2(1)[25,26]	4(14), 43(4)
H_2O	BEVXEF01	glycylaspartic acid dihydrate	$P2_12_12_1$	2.14, 2.08	1.7, 1.4[46]	−21, −33
H_2O		DL-homoproline tetrahydrate	$P2_1/c$	2.17	3.4[47]	57
H_2O	GLYTRE03, GLYTRE04	glycyl-L-threonine dihydrate	$P2_12_12_1$	2.27, 2.07; 2.16	1.6(3), 2.2(8);[48] 1.5(1)[49,50]	−30(13), 6(39); −31(5)
H_2O		L-histidyl-L-alanine dihydrate	$P2_1$	2.11, 2.22	2.5(6), 2.4(6); 2.1(1), 2.3(1)[49,50]	18(28), 8(27); 0(5), 4(5)
H_2O		glycyl-L-histidine dihydrate	$P2_1$	2.21, 2.19	2.4(5), 2.5(5)[49,50]	9(23), 14(23)
H_2O	LTYRGG01	tyrosyl-glycyl-glycine monohydrate	$P2_12_12_1$	2.11	1.7[46]	−19
H_2O		L-phenylalanyl-L-proline monohydrate	$P4_32_12$	2.21	2.8(1)[49,50]	27(5)
H_2O	KESXOV01	3-(1,3-diisopropyl-2-imidazolidinylidene)-2,4-pentanedione monohydrate	$Pna2_1$	2.16	2.5(2)[51]	16(9)
H_2O	CAMVES	cyclo-(DL-prolyl)$_2$-(L-alanyl)$_4$ monohydrate	$P2_12_12_1$	2.22	2.1(1)[49,50]	−5(5)
H_3N		ammonia	$P2_13$	1.69	1.50(6)[52]	−11(4)
H_3NO_3S		sulfamic acid	$Pbca$	8.93	9.9(6)[53,54]	11(7)
CH_2N_2	CENHAE02	18-crown-6 cyanamide complex	$P2_1/c$	4.87	5.54[55]	14
CH_3NO	FORMAM02	formamide	$P2_1/n$	4.57	4.8(5)[54]	5(11)
CH_4N_2O	UREAXX12	urea	$P\bar{4}2_1m$	5.13	5.4(5), 5.7(5);[56,57] 6.2(5)[58]	5(10), 11(10); 21(10)
$C_2H_2N_4O_3$	QOYJOD	5-nitro-2,4-dihydro-3H-1,2,4-triazol-3-one (β-NTO)	$P2_1/c$	1.09	3.2(1)[24]	194(9)
$C_2H_4N_4$	CYAMPD03	2-cyanoguanidine	$C2/c$	9.05	11.2[59]	24
$C_2H_5NO_2$	GLYCIN17	glycine (α form)	$P2_1/n$	12.74	14.9(3)[60]	17(2)
C_2H_5NS	THACEM02	thioacetamide	$P2_1/c$	5.63	9.0(1)[61]	60(1)
$C_2H_5N_3OS$	SOJNAG03	1-formyl-3-thiosemicarbazide	$P2_1/c$	8.00	8.9(4)[62]	11(5)
$C_2H_7NO_3S$	TAURIN05	2-aminoethane sulfonic acid (taurine)	$P2_1/c$	15.65	15.5, 18.0[63]	−1, 15
$C_2H_8NO_4P$	AEPHOS02	phosphorylethanolamine	$P2_1/c$	21.82	13(2)[64]	−40(9)
$C_3H_2N_2O_2S$	GIPVUW02	2,5-diaza-1,6-dioxa-6a-thiapentalene	$P2_1/c$	3.75	2(1)[65]	−47(27)
$C_3H_2N_2O_3$	PARBAC03	parabanic acid	$P2_1/n$	2.65	2.3(3)[66]	−13(11)
$C_3H_4N_2$	IMAZOL06	imidazole	$P2_1/c$	3.96	4.8(6)[56,67]	21(15)
$C_3H_7NO_2$	LALNIN04	L-alanine	$P2_12_12_1$	12.36	13.0(7)[68]	5(6)
$C_3H_7NO_3$	DLSERN12	DL-serine	$P2_1/a$	13.83	12.9(3)[69]	−7(2)
$C_4H_2N_2O_4$	ALOXAN12	alloxan	$P4_12_12$	2.95	0.2(10)[56,70]	−93(34)
$C_4H_3N_3O$	NEDXID02	4-cyanoimidazolium-5-olate	$Pna2_1$	11.49	8.6(10), 11.0(14)[71]	−25(9), −4(12)
$C_4H_3N_3O_4$	NIMFOE01	5-nitrouracil	$Pbca$	5.80	5.5(6)[23]	−5(10)
$C_4H_3N_3O_4$	NIMFOE02	5-nitrouracil	$P2_12_12_1$	5.91	9(1)[23]	52(17)
$C_4H_4N_2OS$	TURCIL02	2-thiouracil	$P\bar{1}$	5.67	10.2(6)[25,26]	80(11)
$C_4H_5N_3O$	CYTOSM03, CYTOSM12	cytosine monohydrate	$P2_1/c$	8.19, 8.12	8.2(15),[72] 8.0(14),[45] 11.1(4)[25,26]	0(18), −2(17), 37(5)
$C_4H_7NO_4$	DLASPA03	DL-aspartic acid	$C2/c$	11.36	13.4(8)[73]	18(7)
$C_4H_8N_2O_3$	ASPARM08, ASPARM09	L-asparagine monohydrate	$P2_12_12_1$	14.38, 14.41	14.3(3),[74] 16.7(12)[69]	−1(2), 16(8)
$C_4H_8N_2O_3$	GLYGLY04	glycylglycine	$P2_1/c$	25.33	27.8(17)[75]	10(7)
$C_4H_9NO_2$	GAMBUT02	γ-aminobutyric acid (GABA)	$P2_1/a$	20.04	13(1)[76]	−35(5)
C_5H_5NO	PYRIDO05	2-pyridone	$P2_12_12_1$	5.20	8.8(19)[77]	69(37)
$C_5H_6N_2O_2$	METURA03	1-methyluracil	$Ibam$	5.53	4.4(22), 6.4(27)[78]	−20(40), 16(49)
$C_5H_9NO_2$	DLPROM02	DL-proline monohydrate	$Pbca$	12.41	16.2(7), 13.4(5);[10] 13.0[79]	31(6), 8(4); 5
$C_5H_9NO_4$	CADVUY01	DL-glutamic acid monohydrate	$Pbca$	11.32	8.2(12)[69]	−28(11)
$C_5H_{11}NO_2$	VALIDL03	DL-valine	$P\bar{1}$	11.67	14.3(4)[69]	23(3)
$C_6H_5NO_3$	MNPHOL03	*m*-nitrophenol	$P2_12_12_1$	6.58	5.28(31)[80]	−20(5)
$C_6H_5NO_3$	MNPHOL17	*m*-nitrophenol	$P2_1/n$	6.53	5.81(20)[81]	−11(3)
$C_6H_5NO_3$	NITPOL02	*p*-nitrophenol (β form)	$P2_1/n$	5.85	21.5[27]	268
$C_6H_5NO_3$	NITPOL03	*p*-nitrophenol (α form)	$P2_1/c$	5.83	18.0[27]	209
$C_6H_6N_2O_2$	NANILI02	*p*-nitroaniline (PNA)	$P2_1/c$	8.10	16.1(9), 15.3(9);[10] 16.1(11), 12.4(10)[11]	99(11), 89(11); 99(14), 53(12)
$C_6H_6N_2O_3$	MNPYDO01	3-methyl-4-nitropyridine-*N*-oxide (POM)	$P2_12_12_1$	0.90	1.06(10)[82,83]	18(11)
$C_6H_6N_2S_2$	FANJOT01	2,2-bis(methylthio)-1,1-ethylenedicarbonitrile	$P2_1/n$	7.77	6(2)[23]	−23(26)
$C_6H_7N_5$	MEADEN02	9-methyladenine	$P2_1/c$	2.55	1.8(10)[56,84]	−29(39)

[a] For the ab initio calculations, molecular structures were taken from crystal structures in the Cambridge Structural Database; REFCODES for these are given, and they do not necessarily coincide with the structure reported in the charge density analysis, as those are not always deposited.

Table 2. Full details of space groups, HF/6-31G(d,p) dipole moments, X-ray-derived dipole moments and enhancements, and references to relevant charge density studies, for data in Figures 1 and 2.

Formula	Refcode	Compound name	Space group	$\mu_{6\text{-}31G(d,p)}$	$\mu_{X\text{-}ray}$	$\%\Delta\mu_{X\text{-}ray}$
$C_6H_9N_3O_2$	DLHIST01	DL-histidine	$P2_1/c$	15.77	29.2(24), 17.2(17);[10] 16.57[85]	85(15), 9(11); 5
$C_6H_{10}N_2O_5$	BEVXEF01	glycyl-L-aspartic acid dihydrate	$P2_12_12_1$	25.80	26.1(39)[46]	1(15)
$C_6H_{11}NO_2$		DL-homoproline tetrahydrate	$P2_1/c$	13.10	16.1[47]	23
$C_6H_{12}N_2O_4$	GLYTRE03, GLYTRE04	glycyl-L-threonine dihydrate	$P2_12_12_1$	25.68, 25.96	23.8(38),[48] 28.6(13)[49,50]	−7(15), 10(5)
$C_7HO_2F_5$	PFBZAC01	pentafluorobenzoic acid	$P\bar{1}$	2.12	4.2(5), 3.8(4)[30]	98(24), 79(19)
$C_7H_6O_3$	SALIAC16	salicylic acid	$P2_1/c$	2.95	8.3(6)[25,26]	181(20)
$C_7H_8N_2O_2$	BAJCIY01	2-methyl-4-nitroaniline (MNA)	Ia	8.24	25(8),[2] 12.4(13)[3]	203(97), 50(16)
$C_7H_8N_2O_2$	TIXQUM01	2-methyl-5-nitroaniline (M5NA)	$P2_1/n$	6.75	10.6(9)[86,87]	57(13)
$C_7H_9N_3S$	BUFGIS01	2-(*N*,*N*-dimethylamino)-2-methylthio-1,1-ethylenedicarbonitrile	$Pna2_1$	10.40	15(2)[23]	44(19)
$C_8N_2F_4$	GEYLOL01	3,4,5,6-tetrafluoro-1,2-benzenedicarbonitrile	$P2_12_12_1$	4.38	6.2(4)[88]	42(9)
$C_8N_2F_4$	JUBKIA01	2,4,5,6-tetrafluoro-1,3-benzenedicarbonitrile	$Pbca$	2.46, 2.48	1.0(4), 1.7(4)[88]	−59(16), −31(16)
$C_8H_5N_3$	PYRCYN06	pyridinium dicyanomethylide	$P2_1mn$	11.02	18.8, 9.8[89]	71, −11
$C_8H_7NO_4$	GADBAP01	1-(2-hydroxy-5-nitrophenyl) ethanone	$Pca2_1$	2.51	9.2(6)[31]	267(24)
C_8H_9NO	VOBTOV02	(*Z*)-*N*-methyl-*C*-phenylnitrone	$Pbca$	4.05	4.9[90]	21
$C_8H_{12}N_2O_2$	NANQUO02	3,4-bis(dimethylamino)-3-cyclobutene-1,2-dione (DMACB)	$P\bar{1}$	9.07, 9.07	16.6(13), 16.2(12)[32]	83(14), 79(13)
$C_8H_{12}N_2O_3$	DETBAA04	5,5-diethyl barbituric acid (barbital)	$C2/c$	0.95	0.7(12)[91]	−26(126)
$C_8H_{12}N_4$	BUFGOY01	2,2-bis(*N*,*N*-dimethylamino)-1,1-ethylenedicarbonitrile	$Pcab$	9.88	5(2)[23]	−49(20)
$C_8H_{12}N_4O_3$		L-histidyl-L-alanine dihydrate	$P2_1$	26.29	12.9(31), 17.5(10)[49,50]	−51(12), −33(4)
$C_8H_{15}N_7O_2S_3$	FOGVIG04	famotidine (form A)	$P2_1/c$	8.17	18.1(7)[33]	122(8)
$C_8H_{15}N_7O_2S_3$	FOGVIG05	famotidine (form B)	$P2_1/n$	9.09	20.8(15)[33]	129(17)
$C_8H_{16}N_2O_3S$	ALAMET01	DL-alanyl methionine	$P2_1/c$	24.46	10.0(5)[92]	−59(3)
$C_9H_6O_2$	COUMAR11	2H-chromene-2-one (coumarin)	$Pc2_1b$	5.86	13.5(12)[26,34]	130(20)
C_9H_6OS	CABYAG01	2H-chromene-2-thione (2-thiocoumarin)	$P2_12_12_1$	6.79	15.2(11)[35]	124(16)
C_9H_6OS	MOCTIH01	2H-thiochromene-2-one (1-thiocoumarin)	Pc	5.85	19.2(19)[26,34]	228(32)
$C_9H_6S_2$	MAJJOX	2H-thiochromene-2-thione (dithiocoumarin)	$P\bar{1}$	6.71	14.1(11)[26]	110(16)
$C_9H_{11}NO_4$	LDOPAS03	L-dopa	$P2_1$	10.99	12(5)[93]	9(45)
$C_9H_{13}N_3O_5$	CYTIDI02	β-cytidine	$P2_12_12_1$	10.83	17.2(41)[72]	59(38)
$C_9H_{14}N_4O_3$		glycyl-L-histidine dihydrate	$P2_1$	25.58	12.3(25)[49,50]	−52(10)
$C_{11}H_8O_3$	GAGSIR03	3-acetylcoumarin (form A)	$P\bar{1}$	5.21, 5.09	7.3(6), 8.8(8)[26,36]	40(12), 73(16)
$C_{11}H_8O_3$	GAGSIR05	3-acetylcoumarin (form B)	$P2_1/n$	5.25	9.7(6)[36]	85(11)
$C_{11}H_{14}N_2O_3$	FUDVUV02	*N*-(4-nitrophenyl)-L-prolinol (NPP)	$P2_1$	6.99	9.6(14)[94,95]	37(20)
$C_{11}H_{14}N_2O_3$		glycyl-DL-phenylalanine	$Pbca$	24.38	20.9(14)[49,50]	−14(6)
$C_{12}H_{10}N_2O_2$	KEFLEM01	*p*-amino-*p*′-nitrobiphenyl (PANB)	$Pca2_1$	9.00	73.5(69), 43.4(51);[10,96] 23.8(42)[28]	717(77), 382(57); 164(47)
$C_{12}H_{10}N_2O_2$	MAWBOB	*p*-amino-*p*′-nitrobiphenyl/triphenylphosphine oxide (PANB/TPPO)	$P\bar{1}$	8.61	16.8(16)[37]	95(19)
$C_{12}H_{12}O_5$	MACLAE	austdiol	$P2_12_12_1$	5.82	4.8(9)[97]	−18(15)
$C_{13}H_{12}N_4O_4$	RIWQET01	2-(methylbenzylamino)-3,5-dinitropyridine (MBADNP)	$P2_1$	5.95	5.6[98]	−6
$C_{13}H_{17}N_3O_5$	LTYRGG01	tyrosyl-glycyl-glycine monohydrate	$P2_12_12_1$	37.35	36.0(39)[46]	−4(10)
$C_{13}H_{18}O_2$	IBPRAC02	*rac*-2-(4-isobutylphenyl)-propionic acid (ibuprofen)	$P2_1/c$	1.91	10.98[38]	475
$C_{14}H_{18}N_2O_3$		L-phenylalanyl-L-proline monohydrate	$P4_32_12$	16.38	20.1(9)[49,50]	23(5)
$C_{14}H_{24}N_2O_2$	KESXOV01	3-(1,3-diisopropyl-2-imidazolidinylidene)-2,4-pentanedione monohydrate	$Pna2_1$	9.19	12.0(29)[51]	31(32)
$C_{18}H_9O_3P$	RICFEO01	phosphangulene	$R3m$	3.35	4.7(25)[99]	40(75)
$C_{18}H_{24}N_4$	ROPPIV	(4-bis(diethylamino)-methylium)phenyl-dicyanomethanide (DED-TCNQ)	$P2_1/c$	23.73	27.3[100]	15
$C_{22}H_{28}N_4O_2$	NATWOU01	7,7-bis(*S*)-(+)-2-(methoxymethyl) pyrrolidino)-8,8-dicyanoquinodimethane (DMPDQ)	$P2_1$	23.08	44(6)[39]	91(26)
$C_{22}H_{34}N_6O_6$	CAMVES	cyclo-(DL-prolyl)$_2$-(L-alanyl)$_4$ monohydrate	$P2_12_12_1$	12.36	23.8(10)[49,50]	93(9)
$C_{23}H_{27}N_5O_2$	FUGQON01	terbogrel	$P2_1/a$	10.90	21.9(16)[41]	101(15)
$C_{32}H_{50}N_6O_9$		Boc-Gln-D-Iva-Hyp-Ala-Phol	$P2_12_12_1$	13.4	18.6[101]	39

[a] For the ab initio calculations, molecular structures were taken from crystal structures in the Cambridge Structural Database; REFCODES for these are given, and they do not necessarily coincide with the structure reported in the charge density analysis, as those are not always deposited.

2) partitioning of a periodic theoretical electron density due to a superposition of non-interacting molecules at the crystal geometry, using either a multipole refinement approach, QTAM, or Hirshfeld surfaces;

3) experimental measurements in solution or (rarely, for molecules of interest) in the gas phase.

All of these approaches have been used in previous studies. For the present analysis, we need to establish a consistent benchmark for the purposes of reviewing a large number of experimental determinations, and hence we concentrate on only the electronic rearrangement relative to a reference isolated-molecule calculation at the geometry observed in the crystal. In practice, we define the dipole moment enhancement relative to the ab initio HF/6-31G(d,p)[18] result for an isolated molecule, using the observed crystal geometry but with X–H bonds set to average neutron-diffraction values.[19] The quantity of interest is the percentage enhancement shown in Equation (1):

$$\%\Delta\mu_{X-ray} = 100(\mu_{X-ray} - \mu_{6-31G(d,p)})/\mu_{6-31G(d,p)} \quad (1)$$

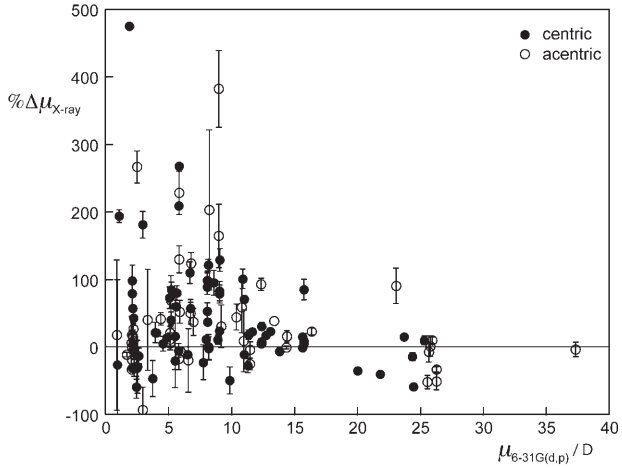

Figure 1. Estimates of enhancement of the molecular dipole moment [Eq. (1)] versus theoretical results computed for isolated molecules at the crystal geometry. The symbols identify results based on X-ray diffraction data for molecules crystallizing in centrosymmetric (●, centric) and non-centrosymmetric (○, acentric) space groups. Error bars represent one estimated standard deviation.

3. Dipole Moments from X-ray Diffraction Data

3.1 An Overview of the Diffraction Results

Tables 1 and 2 summarizes the molecular dipole moments derived from X-ray diffraction data $\mu_{X\text{-ray}}$, from theory $\mu_{6\text{-}31G(d,p)}$, and estimates of the enhancement $\%\Delta\mu_{X\text{-ray}}$, as defined above. In compiling this table we have attempted to include all experimental results based on multipole modeling of the diffraction data, but, in contrast to the earlier review,[4] we have excluded results from monopole-only (kappa) refinements. For that reason, only 18 of the entries in Tables 1 and 2 were included in the earlier review; 85% of the results in Tables 1 and 2 have been reported since that review was published. This makes the present overview much more than a simple update but capable of a rather detailed analysis of trends and identification of significant outliers.

Figure 1 plots $\%\Delta\mu_{X-ray}$ against $\mu_{6\text{-}31G(d,p)}$ for all entries in Tables 1 and 2; error estimates are included if they were reported in the original publications. Where multiple determinations have been made, either from different experimental data sets (e.g. urea) or different multipole models applied to the same X-ray data (e.g. *p*-nitroaniline), separate results have been included. Figure 1 quite clearly shows that molecular dipole moments are enhanced for the majority of molecules, but there are a significant number of cases where the opposite is observed. For the majority of molecules, $\%\Delta\mu_{X-ray}$ lies between -50% and $+100\%$, with a small number of studies reporting results outside this range, most notably large positive enhancements by as much as almost 500%. Furthermore, molecules with large dipole moments tend to display much smaller deviations from the isolated-molecule values. To identify a possible difference between analyses of diffraction data from centrosymmetric (centric) and non-centrosymmetric (acentric) crystal structures, we depict the two sets of points differently in the figure. Contrary to our expectations, there appears to be no correlation between these very large enhancements and non-centrosymmetric space groups.

Figure 2 breaks down the data in a different way and presents a histogram of the frequency of occurrence of enhancement in a particular range (in intervals of 25%), with separate plots for centric and acentric space groups. We see a definite difference between the two categories. For acentric space

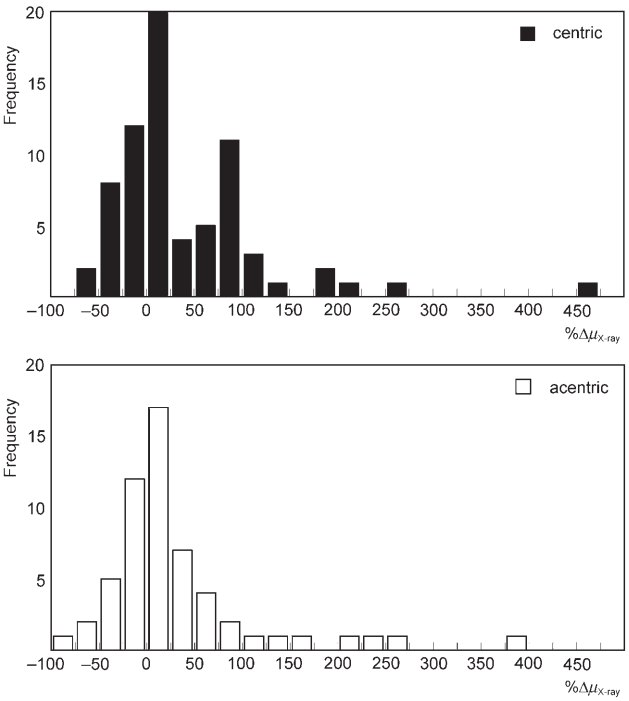

Figure 2. Histograms of frequency of occurrence of dipole moment enhancement for both centric and acentric space groups.

groups, the data is distributed rather nicely about zero, and slightly skewed towards positive enhancement, as expected [in the sense that the definition in Equation (1) ensures that $\%\Delta\mu_{X-ray} \geq -100\%$]. In contrast, the histogram for the centric space groups is distinctly bimodal, with one peak between 0 and 25% and a second one between 75 and 100%. In both cases there are numerous examples of negative enhancement, as well as clear outliers at enhancements of 100% or greater, and again we see no compelling evidence for the assertion that acentric space groups cause special problems [although in both Figures 1 and 2 we have omitted a single point at $\%\Delta\mu_{X-ray} = 717(77)\%$ for *p*-amino-*p*′-nitrobiphenyl (PANB); see Tables 1 and 2 and discussion below]. The spread of data in Figure 2 suggests a way to identify outliers for closer examination by establishing a reasonable range for enhancement, taking into account the often quite large estimated errors. We choose $\pm 75\%$ as this cutoff and discuss in some detail below those studies for which $\%\Delta\mu_{X-ray}$ is significantly different from zero and beyond $\pm 75\%$.

3.2 Using Theory to Benchmark X-ray Diffraction Results

Before discussing each of the outliers in turn, we need to establish criteria for deciding whether a particular result is physically reasonable or not; we need some benchmarks against which to judge the X-ray diffraction results, and, if possible, we need an independent method which is readily applicable to each one. As discussed in Section 2.2, crystal electron densities must be partitioned into molecular fragments and the resulting dipole moments compared with those obtained from a similar partitioning of a sum of isolated (non-interacting) molecules. Thus, for a subset of molecules in Tables 1 and 2, we performed PHF calculations with CRYSTAL98[20] using a polarized double zeta (DZP) basis set;[21] using the MOLSPLIT option yielded electron distributions arising from a sum of non-interacting molecules. Following the procedures outlined in detail elsewhere,[17] molecular dipole moments were obtained using two distinctly different partitioning schemes to define molecular regions: Hirshfeld surfaces[16] and Bader's QTAM.[13] For the former case, the crystalline electric field and electrostatic potential were computed at points on Hirshfeld surfaces around each molecule, obtained at a resolution of 10 points/au, and surface integration was used to determine molecular dipole moments. For the latter case, QTAM atomic charges and dipole moments were obtained from the periodic electron distributions using TOPOND,[22] from which molecular dipole moments were computed by appropriate summation.

Table 3 summarizes the results for 11 molecular crystals ranging in size from formamide to PANB. The results emphasize the nonuniqueness of molecular dipole moments in crystals but, most importantly for our purposes, the estimated enhancements are mostly independent of the choice of partitioning scheme. It can be seen that the smaller magnitude of dipole moment enhancements in Table 3 compared with Tables 1 and 2 is not related to the different choice of reference in the two cases, as the QTAM "molecules" values in Table 3 are quite similar to the HF/6-31G(d,p) values in Tables 1 and 2. We believe that the molecular dipole implied by a superposition of non-interacting molecules in the same crystal geometry is a better reference than the result from a calculation on an isolated molecule, where the ambiguity of gas-phase or crystal geometry exists. A striking outcome from these theoretical results is that none of the enhancements is particularly large: all are within the range $\pm 50\%$, which is somewhat at odds with the experimental results listed in Tables 1 and 2. Thus, theory predicts a modest enhancement

Table 3. Molecular dipole moments and percentage enhancements from theory. Hirshfeld surface and QTAM columns result from space partitioning of PHF/DZP electron densities for a superposition of molecules and for the crystal. Lorentz factor tensor results refer to the self-consistent polarization of HF/6-31G(d,p) wavefunctions using electric fields obtained from dipole lattice summation in the crystal.

	Hirshfeld surface			QTAM			Lorentz factor tensors[a]					Experiment
Compound	Molecules	Crystal	$\%\Delta\mu_{HS}$	Molecules	Crystal	$\%\Delta\mu_{QTAM}$	μ_0	μ_∞	$\%\Delta\mu_{LT}$	$\lvert F_0 \rvert$ [GV m^{-1}]	θ [deg]	$\%\Delta\mu_{X\text{-}ray}$
formamide	3.54	4.72	33	4.71	6.14	30	4.57	5.78	26	7.4	1	5(11)[54]
urea	3.79	5.19	37	5.31	7.01	32	5.13	6.29	23	6.5	0	5(10), 11(10);[56,57] 21(10)[58]
β-NTO	1.39	0.84	−40	1.14	0.62	−46	1.09	1.26	16	1.0	76	194(9)[24]
glycine	10.15	11.66	15	13.11	15.09	15	12.74	15.76	24	15.5	16	17(2)[60]
5-nitrouracil[b]	5.13	7.24	41	6.20	8.54	38	5.80	7.00	21	2.2	6	18(7)[23]
5-nitrouracil[c]	5.14	6.90	34	6.22	8.67	39	5.91	6.75	14	2.5	52	52(17)[23]
β-4-nitrophenol[d]	4.32	5.83	35	6.10	7.59	24	5.85	7.11	22	2.4	43	268[27]
α-4-nitrophenol	4.36	5.49	26	6.37	7.74	22	5.83	7.62	31	2.6	18	209[27]
MNA	6.88	9.33	36	8.98	11.72	31	8.24	11.25	37	3.3	12	203(97),[2] 50(16)[3]
ethanone	2.24	2.11	−6	2.48	2.42	−2	2.51	3.13	25	0.9	24	267(24)[31]
PANB	7.53	8.97	19	9.20	10.81	18	9.00	11.35	26	1.4	7	717(77), 382(57);[10,96] 164(47)[28]

[a] μ_0 is the zero-field dipole moment, the same quantity as $\mu_{6\text{-}31G(d,p)}$ in Tables 1 and 2. μ_∞ is the molecular dipole moment after convergence of the iterative polarization to self-consistency (i.e. when the dipole moment of the polarized molecule is the same as that of the surrounding molecules generating the electric field). $\lvert F_0 \rvert$ is the magnitude of the polarizing field produced by the zero-field molecular dipoles, and θ is the angle between this field and the zero-field dipole moment. [b] centrosymmetric polymorph. [c] non-centrosymmetric polymorph. [d] both forms are centrosymmetric.

of ≈20% for PANB (far less than any experimental result), an enhancement of ≈35% for MNA (in contrast to the widely cited original result, but in excellent agreement with our recent redetermination),[3] and almost no change for 1-(2-hydroxy-5-nitrophenyl)ethanone. Similarly, the pronounced enhancements of more than 200% inferred from X-ray data for the polymorphs of 4-nitrophenol are not supported by the ab initio calculations, which instead predict small enhancements in the range of 25–35%. For 5-nitro-2,4-dihydro-3H-1,2,4-triazol-3-one (β-NTO), the experimental result implied an enhancement near 200%, but both partitioning schemes predict quite the opposite: a small decrease in the dipole moment of ≈0.50 D. Finally, all theoretical approaches fail to support the experimental differences observed between the polymorphs of 5-nitrouracil, one centrosymmetric for which a negligible dipole moment enhancement is observed and the other non-centrosymmetric for which an enhancement of ≈50% is indicated. As the molecular structure is identical in the two crystal structures, this result has been regarded as a convincing demonstration of the effects of the different intermolecular interactions in the two polymorphs, one displaying hydrogen-bonded cyclic dimers and the other linear chains.[1,23] However, if the reported experimental errors are regarded as realistic, then neither polymorph can be ascribed a significant dipole moment enhancement at the 3σ level of confidence.

Given the large number of outliers (more than 20 molecular crystals), some of quite substantial size, it is clearly not always possible—or desirable—to perform these calculations routinely. A simpler approach has been described recently that takes advantage of Lorentz factor tensors (dipole lattice sums) to estimate the electric field in a crystal arising from point dipoles of surrounding molecules; this field is then applied iteratively to polarize a molecule in a self-consistent manner (i.e. until the dipole moment of the polarized molecule is the same as that of the surrounding polarizing molecules).[5] For these calculations we use wavefunctions at the HF/6-31G(d,p) level with identical molecular geometries to those used earlier. The dipole moment enhancement is then estimated from the difference between the zero-field value ($\mu_0 = \mu_{6-31G(d,p)}$, Tables 1 and 2) and the value obtained at convergence of the iterative process (usually four or five cycles), $\%\Delta\mu_{LT} = 100(\mu_\infty - \mu_0)/\mu_0$. The results (Table 3) demonstrate that this relatively straightforward approach represents a viable route to estimating molecular dipole moment enhancement in crystals. Typical enhancements are in the range of 10–40%, often agreeing well with results from partitioning of crystal Hartree–Fock electron densities; as expected, agreement is not perfect, since the effects of important intermolecular interactions, such as hydrogen bonding, are ignored completely. However, the Lorentz factor tensor approach also provides an estimate of the magnitude of the average electric field experienced by each molecule in the crystal and, of equal importance, of the angle it forms with respect to the zero-field dipole moment. In this manner the dipole moment enhancement can be rationalized in terms of field magnitude, direction, and molecular polarizability (which correlates roughly with molecular size).

3.3 Significant X-ray Diffraction Enhancements Outside the Range ±75%

In this section, we discuss the outliers identified from Figure 2 and Tables 1 and 2. These are the molecules for which $\%\Delta\mu_{X-ray}$ is significantly different from zero (i.e. $|\%\Delta\mu_{X-ray}| > 3\sigma$) and outside the cutoff of ±75%. Where no estimate of error has been provided, we discuss the result nevertheless. Tables 3 and 4 report theoretical estimates of dipole moment enhancement, from either Hirshfeld surface or QTAM partitioning of the PHF electron distribution or based on Lorentz factor tensor analysis, for all outliers with the exception of 3,4-bis(dimethylamino)-3-cyclobutene-1,2-dione (DMACB). This molecular crystal has two molecules in the asymmetric unit and cannot presently be treated with our implementation of the Lorentz factor tensor approach.[5] However, QTAM results

Table 4. Molecular dipole moments and percentage enhancement from Lorentz factor tensor analysis, compared with experimental results for outliers in Figure 2 (see text for detailed discussion of each outlier).

Compound	Lorentz factor tensors[a]					Experiment
	μ_0	μ_∞	$\%\Delta\mu_{LT}$	$\lvert\mathbf{F}_0\rvert$ [GV m^{-1}]	θ [deg]	$\%\Delta\mu_{X-ray}$
2-thiouracil	5.67	5.85	3	3.9	100	80(11)[25,26]
p-nitroaniline	8.10	10.85	34	3.3	14	99(11), 89(11);[10] 99(14), 53(12)[11]
DL-histidine	15.77	18.26	16	5.1	9	85(15), 9(11);[10] 5[85]
pentafluorobenzoic acid	2.12	2.18	3	0.8	92	98(24), 79(19)[30]
salicylic acid	2.95	3.63	23	1.4	24	181(20)[25,26]
famotidine A	8.17	10.55	29	2.2	15	122(8)[33]
famotidine B	9.09	12.23	35	3.9	53	129(17)[33]
coumarin	5.86	7.87	34	2.7	23	130(20)[26,34]
2-thiocoumarin	6.79	6.82	1	2.0	92	124(16)[35]
1-thiocoumarin	5.85	7.70	32	2.1	24	228(32)[26,34]
dithiocoumarin	6.71	9.81	46	2.0	7	110(16)[26]
3-acetylcoumarin (form B)	5.25	5.45	4	1.3	83	85(11)[36]
ibuprofen	1.91	1.38	−28	1.3	160	475[38]
DMPDQ	23.08	30.18	31	3.1	15	91(26)[39]
cyclo-(DL-prolyl)$_2$-(L-alanyl)$_4$ monohydrate	12.36	17.60	42	3.5	15	93(9)[49,50]
terbogrel	10.90	9.58	−12	2.3	126	101(15)[41]

[a] μ_0 is the zero-field dipole moment, the same quantity as $\mu_{6\text{-}31G(d,p)}$ in Tables 1 and 2. μ_∞ is the molecular dipole moment after convergence of the iterative polarization to self-consistency (i.e. when the dipole moment of the polarized molecule is the same as that of the surrounding molecules generating the electric field). $|\boldsymbol{F}_0|$ is the magnitude of the polarizing field produced by the zero-field molecular dipoles, and θ is the angle between this field and the zero-field dipole moment.

were published in the original experimental study, and these form the basis of comparison for that system.

β-NTO: The experimental enhancement of 194(9)%[24] is not supported by any of the theoretical estimates in Table 3, and dipole moments obtained by partitioning a PHF electron density predict a substantial negative enhancement, while the Lorentz tensor result is a modest increase. NTO is a small five-membered heterocycle with N–H, C=O, and $-NO_2$ functional groups, and as such, its small dipole moment results from the vector sum of quite large contributions from these functional groups. The crystal electric field is predicted to make an angle of 76° with the zero-field dipole.

2-Thiouracil: This molecule is similar in some respects to NTO, with C=S, N–H, and C=O groups around a six-membered heterocycle, although μ_0 in this case is larger. The experimental enhancement of 80(11)%[25,26] is in disagreement with the Lorentz tensor estimate of 3%, a result that originates from the near orthogonality of the crystal electric field to the zero-field dipole.

***p*-Nitrophenol:** Both polymorphs crystallize in centrosymmetric space groups, and the charge density studies yield similar results for both forms, thus suggesting substantial dipole moment enhancements (268 and 209%) for this molecule from two quite separate experimental studies;[27] no experimental errors were reported for these quantities. In this case, the partitioning of PHF electron densities and Lorentz tensor estimates are in agreement; they all predict an enhancement of between 22 and 35%.

***p*-Nitroaniline (pNA):** No detailed charge density study has been published for this compound, but several different multipole refinements of the 20 K synchrotron data have been published by Coppens and co-workers,[10,11,28] all of which suggest an enhancement in the range of 50–100%. As also discussed for PANB (see below), the highest of these values results partly from a lack of physical constraints in the refinement, and this led Coppens and co-workers to favor the use of the κ′-restricted multipole model (KRMM),[10] where scaling factors for higher multipole radial functions are fixed at values derived from fits to theoretical structure factors. The KRMM method results in a dipole moment of 12.4(10) D, in excellent agreement with QTAM partitioning of PHF/6-31G(d,p) and PDFT/6-31G(d,p) electron densities (11.2 and 11.8 D, respectively).[11] These theoretical values are also in excellent agreement with the Lorentz factor tensor result of $\mu_\infty = 10.9$ D. For this centrosymmetric crystal there is, therefore, quite general agreement on the magnitude of the in-crystal dipole moment and an enhancement of 35–50%, depending on the chosen reference value.

DL-Histidine: This is another example where the KRMM yields a much smaller dipole moment [17.2(17) D] than the unrestricted model [29.2(24) D].[10] Although the latter result suggests an enhancement of 85(15)%, the KRMM result implies almost no enhancement, in accord with the Lorentz tensor approach, which yields $\mu_\infty = 18.3$ D, a 16% enhancement. QTAM partitioning of a PHF/6-21G(d,p) electron density reported by Volkov[29] yielded a dipole moment of 19.9 D. It is noteworthy that this relatively modest enhancement occurs despite the rather large crystal electric field of 5.1 GV m^{-1}, directed almost parallel to the molecular dipole. As remarked previously for glycine,[17] amino acids such as this that exist in zwitterionic form in the crystal generate large electric fields because of their substantial dipole moments, but this does not translate into very large dipole enhancements, principally because the molecules are already highly polarized. We elaborate a little further on this observation below.

Pentafluorobenzoic Acid: Bach et al. performed two different multipole refinements of this 110 K laboratory data, which differed only in the assumed symmetry of deformations on the F, C, and O atoms.[30] The dipole moments that result are not significantly different from one another and suggest an enhancement of 80–100%. This result is clearly not supported by the Lorentz tensor calculation, which predicts a negligible enhancement from the combination of a small crystal field nearly orthogonal to the molecular dipole. We note that the error estimates on the experimental quantities are relatively large, and as such the experimental results are not entirely inconsistent with the Lorentz tensor estimate.

Salicylic Acid: Like pentafluorobenzoic acid, salicylic acid forms centrosymmetric, hydrogen-bonded dimers in the crystal. The enhancement of 181(20)% implied by the experimental dipole moment[25,26] is far greater than the Lorentz tensor prediction, and given the relatively small error estimate, this result needs to be re-examined.

2-Methyl-4-nitroanline (MNA): As discussed in the Introduction, the pronounced enhancement of the dipole moment observed for MNA by Howard et al. (203(97)%)[2] has been widely cited, but a recent careful experimental study based on new X-ray and neutron diffraction data[3] resulted in $\mu_{X-ray} = 12.4(13)$ D and a much lower $\%\Delta\mu_{X-ray} = 50(16)\%$. This more recent result is in excellent agreement with all theoretical estimates in Table 3, and the Lorentz tensor results show that this considerable enhancement is the result of a substantial electric field in the crystal (3.3 GV m^{-1}) nearly parallel to the molecular dipole. As for pNA, we regard this substantial agreement between experiment and theory as confirmation that the enhancement for MNA is in the range of 35–50%.

1-(2-Hydroxy-5-nitrophenyl)ethanone: Although the charge density study of Hibbs et al. incorporated neutron diffraction results to describe the thermal motion of the H atoms,[31] the theoretical estimates of dipole enhancement in Table 3 (−6, −2, and 25%) are in complete disagreement with the experimental result of 267(24)%. The Lorentz tensor calculations suggest that the crystal electric field at the molecule is rather modest, and it seems unlikely that the enhancement is as large as obtained from the X-ray diffraction data. A re-examination of this result is required, and we note that the space

group for this molecular crystal is not only acentric but polar, as well.

3,4-Bis(dimethylamino)-3-cyclobutene-1,2,-dione (DMACB): The charge density study for DMACB was based on 20 K laboratory data, and anisotropic thermal motion was included in the modeling process for all H atoms.[32] There are two independent molecules in the asymmetric unit for which the experimental estimates of μ_{X-ray} agree well, thus suggesting an enhancement of $\approx$80(13)% relative to an isolated molecule in the same geometry. This result was the subject of considerable discussion by May et al.,[32] since the crystal structure lacks typical hydrogen bonds (although there are a large number of C–H···O interactions). QTAM partitioning of a PHF/6-21G electron distribution in the original study suggested enhancements of 50 and 54% for the two independent molecules, again with respect to isolated molecules. Unfortunately, at present our Lorentz tensor approach is limited to crystals with one independent molecule in the asymmetric unit and cannot be applied to DMACB. However, based on the large zero-field dipole moment of $\approx$9 D, a large dipole moment enhancement can be readily rationalized if the resulting electric field experienced by the molecules is closely aligned with the molecular dipole. The fact that the two DMACB molecules pack alternately in rows to form polar layers, with an angle of $\approx 50^\circ$ between the molecular dipoles in alternating rows, suggests that this will be the case. Given that the enhancement has been attributed to the large number of C–H···O interactions, with no mention of the likely polarization due to the surrounding crystal field (i.e. ignoring the specific intermolecular interactions), it would be worthwhile investigating this system in more detail.

Famotidine: The two polymorphs of famotidine studied by Overgaard and Hibbs[33] are quite distinct conformational isomers, which explains the difference between $\mu_{6-31G(d,p)}$ for the two structures (Tables 1 and 2). The X-ray-derived dipole moments are large for both forms and imply enhancements of $\approx$125(15)%. Such a large enhancement is not supported by the Lorentz tensor results (Table 4), which predict enhancements of 29% for form A and 35% for form B. Curiously, the difference of 15% between μ_{X-ray} for the two forms, with form B having the higher value, is closely reproduced by the Lorentz tensor calculations. Both forms crystallize in centrosymmetric space groups, and we can find no explanation (or support) for the large enhancements obtained experimentally.

Coumarin, 1-Thiocoumarin, 2-Thiocoumarin, and Dithiocoumarin: This series of related molecules has been studied by Munshi and Guru Row,[26,34,35] with multipole refinements based on 90 K laboratory data; three of the four compounds crystallize in acentric space groups, two of which are polar (coumarin and 1-thiocoumarin). As was the case for DMACB, these molecules are devoid of functional groups that normally lead to strong hydrogen bonds, but despite this, pronounced dipole moment enhancements of between 110(16) and 228(32)% are obtained experimentally. None of these results is supported by our Lorentz tensor estimates (Table 4). However, for all of these molecules except 2-thiocoumarin, the method predicts quite large enhancements of between 32 and 46%. The predicted value of 46% for dithiocoumarin is the largest we have obtained with this approach and results from a favorable alignment of the crystal field with the molecular dipole, coupled with what is likely to be a large in-plane polarizability for this molecule.

3-Acetylcoumarin: The two polymorphs are centric, with charge density studies based on 90 K laboratory data; form A has two independent molecules in the asymmetric unit.[36] Lorentz factor tensor calculations on form B do not support the large enhancement reported experimentally [85(11)%], instead predicting a negligible change from the zero-field value as a result of both a small crystal field and an unfavorable alignment.

PANB: The three experimental results for PANB are based on multipole refinements against the same synchrotron data measured at 20 K, but they differ in their treatment of the radial parameters. Abramov et al.[10] acknowledge that the highest of these values represents an unrealistic enhancement, resulting partly from a lack of physical constraints in the refinement and partly from the variability of reflection phases for this acentric polar space group. Along with the result for pNA, this outcome for PANB led Coppens and co-workers to favor use of KRMM refinements. We note that the smallest experimental estimate of 23.8(42) D resulted from "an improved charge density model,"[28] although no details were provided in that work. The theoretical estimates of enhancement in Table 3 lie between 18 and 26%, far below even the lowest experimental estimate, and from the Lorentz tensor results we see that, despite the relatively large zero-field dipole and its favorable alignment with the crystal field, the field is rather modest at 1.4 GV m^{-1}, presumably because of the large separation between point dipoles in this case. Our QTAM dipole moment of 10.9 D (based on a PHF/DZP electron density) essentially agrees with that reported by Volkov[29] (11.3 D, based on a PHF/6-31G(d,p) electron density), but not with the earlier value of 23.0 D reported for QTAM partitioning of a PHF/6-21G(d,p) electron density,[10] a result which now appears to be in error. A detailed reappraisal of the multipole refinement modeling for this compound seems in order, with the aim of identifying the precise contributions to such large discrepancies between experiment and theory. A separate measurement of the PANB dipole moment has been reported for a PANB/triphenylphosphine oxide (TPPO) complex;[37] the result of 16.8(16) D suggests an enhancement of 95(19)%, but at present we cannot benchmark this result against a Lorentz tensor calculation.

Ibuprofen: We suspect the experimental dipole moment of 10.98 D,[38] implying an enhancement of 475% for ibuprofen, is in error, as the molecule is essentially a hydrocarbon with a terminal –COOH group and hence highly unlikely to be as polar as suggested by the X-ray experiment. The Lorentz tensor approach predicts a modest crystal electric field and a negative enhancement of –28%.

7,7-Bis(*S*-(+)-2-(methoxymethyl)pyrrolidino)-8,8-dicyanoquinodimethane (DMPDQ): This large molecule with nonlinear optical potential crystallizes in an acentric polar space group, and the multipole refinement based on laboratory data measured at 130 K[39] implies an enhancement of 91(26)%. Although this result has a large relative error, the Lorentz tensor approach certainly supports the case for a significant enhancement, but closer to 30% and arising from the large crystal field aligned favorably with the molecular dipole.

Cyclo-(DL-prolyl)$_2$-(L-alanyl)$_4$ Monohydrate: The experimental charge density study of this cyclic hexapeptide by Dittrich et al.[40] is based on 100 K synchrotron data and predicts a substantial and significant enhancement of 93(9)%. The Lorentz tensor approach using only point dipoles for the hexapeptide (i.e. ignoring the water molecules) predicts a relatively large enhancement of 42%, which results from a substantial crystal field aligned nearly parallel with the molecular dipole. It is conceivable that the effects of hydrogen bonding will further increase the dipole moment in the crystal, and we therefore cannot rule out an enhancement of more than 50%.

Terbogrel: This molecule is of a similar size to the cyclic hexapeptide above, and the isolated-molecule theory predicts only a slightly smaller dipole moment than for the hexapeptide. However, Lorentz tensor estimates differ considerably, and a small negative enhancement is predicted due to an angle of $\approx 120^\circ$ between the crystal field and the molecular dipole, in disagreement with the experimental estimate of 101(15)%.[41]

3.4 Trends for Amino Acids and Peptides

Tables 1 and 2 include a large number of results for these important materials: ten amino acids, eight dipeptides, and three polypeptides (although more studies than this have been reported that do not provide dipole moment estimates). All amino acids and peptides exhibit quite large X-ray-derived dipole moments in the crystal, with values between 8.2 and 36.0 D, but for almost all of these the enhancement over the isolated-molecule result is very small or negligible. The majority are zwitterionic in the crystal, with dipole moments dominated by large net charges on $-COO^-$ and $-NH_3^+$ groups and, because of this, polarization of the electron density in the crystal is a small perturbation in most cases. The bulk of studies on amino acids and dipeptides (12 of the total of 18) have been performed on achiral molecules or racemic mixtures, and because of their tendency to display small enhancements, this sample contributes significantly to the bars between −25% and 0% and between 0% and 25% in the centric histogram in Figure 2.

A notable exception with a large apparent reduction in dipole moment [−59(3)%] is alanylmethionine, although this result is not supported by a Lorentz tensor analysis, which suggests a small enhancement of 16%. It may not be coincidental that it is the only amino acid or peptide containing a sulfur atom, for which the choice of suitable radial functions has been problematic.[42] Another exception is the hexapeptide cyclo-(DL-prolyl)$_2$-(L-alanyl)$_4$, where an enhancement of 93(9)% is observed; in this case the polypeptide is not zwitterionic.

4. Summary and Outlook

We have collated all known experimental determinations of molecular dipole moments based on multipole modeling of X-ray diffraction data and used this database to identify broad trends in the enhancements implied by the measurements as well as outliers for which apparent enhancements are much greater than 75%. The considerable number of experimental determinations now available has enabled us to pinpoint those studies which merit further attention, either because they seem to point unequivocally to a considerable enhancement in the crystal (e.g. pNA, MNA, and DMACB) or because the reported experimental values are much larger than independent theoretical calculations would suggest. In both cases, further detailed experimental and theoretical studies are indicated, as they are likely to provide considerable insight into the factors that lead to large dipole moment enhancements, especially clarifying the separate roles of the crystal field and hydrogen bonding, and to identify unambiguously those aspects of the multipole refinement procedure (not just the multipole model) that may be improved to obtain reliable results in a more routine manner. A number of important conclusions emerge.

It would seem that any pronounced enhancement, especially greater than 100% relative to an isolated-molecule result at the same geometry, should be regarded with considerable scepticism and certainly not accepted at face value. At the very least, any result of this kind should be compared with periodic ab initio results or Lorentz factor tensor estimates, in a manner similar to that used here, or with independent experimental measurements in solution, if available. The theoretical results may not be definitive, especially because the very definition of a molecule in a crystal is ambiguous, but they will be strongly indicative.

Of the outliers discussed in Section 3.3, in all cases except three—MNA, DMACB, and 1-(2-hydroxy-5-nitrophenyl)ethanone—the modeling procedure treated thermal motion for the hydrogen atoms as isotropic. It should be more widely recognized that, because hydrogen atoms generally lie on the periphery of organic molecules, they play a significant role in determining properties such as molecular dipole moments and electrostatic potentials. The usual approach in almost 80% of current charge density analyses of X-ray diffraction data on organic molecules is to model their thermal motion as isotropic,[43] with thermal parameters obtained by a spherical-atom refinement using low-angle diffraction data. X–H bond lengths are set to standard neutron diffraction results, and H-atom electron densities are typically described with a monopole and a single bond-directed dipole function. Moreover, the radial scaling parameter for these deformation functions is almost always fixed at a standard value of 1.2, despite the fact that it is well known that radial scaling parameters, isotropic thermal parameters, and atomic charges correlate strongly. This has long been known to be an unsatisfactory situation, and it is

imperative that this treatment be improved in future quantitative charge density analyses seeking detailed information on molecular properties.

There seems to be little correlation between the quality of dipole moments from charge density modeling and the presence of a center of symmetry in the crystal; artifacts clearly arise in modeling irrespective of the space-group symmetry, although it is evident that some non-centrosymmetric space groups can greatly exacerbate known difficulties and ambiguities associated with the multipole refinement. In this context, we note that of the 24 outliers discussed in Section 3.3, 16 crystallize in centric space groups, and of those occurring in the remaining eight acentric space groups, six are polar. Contrary to our initial expectations and to a number of statements in the literature, both the experimental and theoretical results suggest that although a positive enhancement of the molecular dipole moment can be expected to be generally observed upon the formation of a crystal, it is not a necessary consequence of intermolecular interactions and crystal field effects, even where strong hydrogen bonding is involved.

Error estimates are vitally important as they facilitate a realistic assessment of the reliability of experimental values. They must be based on a full-matrix least-squares covariance matrix, and where error estimates are origin-dependent, a sensible and logical choice of origin is the center of mass.[4] When a neutrality constraint is imposed on a molecule in the modeling process, which is most often the case, the error is origin-independent.[12]

Although reliable determination of the molecular dipole moment from modern charge density analyses is well-known to be a challenging undertaking, even with the high quality of diffraction data now obtained on a routine basis, these quantities are increasingly common outcomes of charge density analyses. However, it is still uncommon to find a detailed and critical discussion of molecular dipole moments in those studies that do report them, and many recent studies do not report dipole moments, even where they could have been readily obtained from the model electron distribution. It is worth emphasizing that modern charge density experiments are unrivalled in their potential to provide this information in such a detailed fashion and hence provide insight into the effects of intermolecular interactions and the crystal field arising from neighboring molecules. For this reason they deserve to be exploited to a much greater extent than they have been to date. Herein, we have provided compelling evidence that when due care is taken to avoid systematic errors and modeling artifacts, molecular dipole moments from X-ray diffraction data can provide a wealth of experimental information on the change in the molecular charge distribution that results from crystal formation. As examples we point to the studies on pNA, MNA, DL-histidine, and DMACB, where X-ray diffraction results are in accord with various theoretical estimates. However, it is also equally clear that the current standard practice in charge density studies is not yet capable of yielding unequivocal results, and we have identified several improvements that can be implemented. We hope that this analysis will provide impetus for the incorporation of these improvements on a routine basis and will encourage more researchers to report and discuss molecular dipole moments as part of their charge density studies on molecular crystals.

Acknowledgements

We gratefully acknowledge financial support from the Australian Research Council, and a grant of computer time from iVEC, Western Australia.

Keywords: ab initio calculations · charge density analysis · dipole moment · electron density · X-ray diffraction

[1] T. S. Koritsanszky, P. Coppens, *Chem. Rev.* **2001**, *101*, 1583 – 1627.
[2] S. T. Howard, M. B. Hursthouse, C. W. Lehmann, P. R. Mallinson, C. S. Frampton, *J. Chem. Phys.* **1992**, *97*, 5616 – 5630.
[3] A. E. Whitten, P. Turner, W. T. Klooster, R. O. Piltz, M. A. Spackman, *J. Phys. Chem. A* **2006**, *110*, 8763 – 8776.
[4] M. A. Spackman, *Chem. Rev.* **1992**, *92*, 1769 – 1797.
[5] M. A. Spackman, P. Munshi, D. Jayatilaka, *Chem. Phys. Lett.* **2007**, *443*, 87 – 91.
[6] N. K. Hansen, P. Coppens, *Acta Crystallogr., Sect. A: Found. Crystallogr.* **1978**, *A34*, 909 – 921.
[7] F. L. Hirshfeld, *Acta Crystallogr., Sect. B: Struct. Sci.* **1971**, 27, 769 – 781.
[8] R. F. Stewart, *J. Chem. Phys.* **1973**, *58*, 1668 – 1676.
[9] R. F. Stewart, *Acta Crystallogr., Sect. A: Found. Crystallogr.* **1976**, 32, 565 – 574.
[10] Y. A. Abramov, A. V. Volkov, P. Coppens, *Chem. Phys. Lett.* **1999**, *311*, 81 – 86.
[11] A. Volkov, C. Gatti, Y. Abramov, P. Coppens, *Acta Crystallogr., Sect. A: Found. Crystallogr.* **2000**, *56*, 252 – 258.
[12] P. Coppens, A. Volkov, Y. Abramov, T. Koritsanszky, *Acta Crystallogr., Sect. A: Found. Crystallogr.* **1999**, *55*, 965 – 967.
[13] R. F. W. Bader, *Atoms in Molecules—A Quantum Theory*, Oxford University Press, Oxford, **1990**.
[14] R. F. Stewart, in *The Application of Charge Density Research to Chemistry and Drug Design* (Eds.: G. A. Jeffrey, J. F. Piniella), Plenum Press, New York, **1991**, pp. 63 – 102.
[15] F. L. Hirshfeld, *Theoretica Chimica Acta* **1977**, *44*, 129 – 138.
[16] M. A. Spackman, P. G. Byrom, *Chem. Phys. Lett.* **1997**, *267*, 215 – 220.
[17] A. E. Whitten, C. J. Radford, J. J. McKinnon, M. A. Spackman, *J. Chem. Phys.* **2006**, *124*, 074106.
[18] Gaussian 03 (Revision C.02), M. J. Frisch, G. W. Trucks, H. B. Schlegel, G. E. Scuseria, M. A. Robb, J. R. Cheeseman, J. A. Montgomery, T. Vreven, K. N. Kudin, J. C. Burant, J. M. Millam, S. S. Iyengar, J. Tomasi, V. Barone, B. Mennucci, M. Cossi, G. Scalmani, N. Rega, G. A. Petersson, H. Nakatsuji, M. Hada, M. Ehara, K. Toyota, R. Fukuda, J. Hasegawa, M. Ishida, T. Nakajima, Y. Honda, O. Kitao, H. Nakai, M. Klene, X. Li, J. E. Knox, H. P. Hratchian, J. B. Cross, V. Bakken, C. Adamo, J. Jaramillo, R. Gomperts, R. E. Stratmann, O. Yazyev, A. J. Austin, R. Cammi, C. Pomelli, J. W. Ochterski, P. Y. Ayala, K. Morokuma, G. A. Voth, P. Salvador, J. J. Dannenberg, V. G. Zakrzewski, S. Dapprich, A. D. Daniels, M. C. Strain, O. Farkas, D. K. Malick, A. D. Rabuck, K. Raghavachari, J. B. Foresman, J. V. Ortiz, Q. Cui, A. G. Baboul, S. Clifford, J. Cioslowski, B. B. Stefanov, G. Liu, A. Liashenko, P. Piskorz, I. Komaromi, R. L. Martin, D. J. Fox, T. Keith, M. A. Al-Laham, C. Y. Peng, A. Nanayakkara, M. Challacombe, P. M. W. Gill, B. Johnson, W. Chen, M. W. Wong, C. Gonzalez, J. A. Pople, Gaussian, Inc., Wallingford CT, **2004**.
[19] F. H. Allen, O. Kennard, D. G. Watson, L. Brammer, A. G. Orpen, R. Taylor, in *International Tables for Crystallography, Vol. C* (Ed.: A. J. C. Wilson), Kluwer Academic, Dordrecht, **1995**, pp. 685 – 706.
[20] R. Dovesi, V. R. Saunders, C. Roetti, M. Causa, N. Harrison, R. Orlando, E. Apra, *CRYSTAL98—Users Manual*, 1.0 ed., Theoretical Chemistry Group of Torino, Italy, and CCLRC Daresbury Laboratory, England, **1998**.
[21] A. J. Thakkar, T. Koga, M. Saito, R. E. Hoffmeyer, *Int. J. Quant. Chem. Quant. Chem. Symp.* **1993**, *27*, 343 – 354.
[22] C. Gatti, *TOPOND-98 Users Manual*, **1998**.

[23] R. S. Gopalan, G. U. Kulkarni, C. N. R. Rao, *ChemPhysChem* **2000**, *1*, 127 – 135.
[24] E. A. Zhurova, A. A. Pinkerton, *Acta Crystallogr., Sect. B: Struct. Sci.* **2001**, *57*, 359 – 365.
[25] P. Munshi, T. N. Guru Row, *Acta Crystallogr., Sect. B: Struct. Sci.* **2006**, *62*, 612 – 626.
[26] P. Munshi, T. N. Guru Row, unpublished results.
[27] G. U. Kulkarni, P. Kumaradhas, C. N. R. Rao, *Chem. Mater.* **1998**, *10*, 3498 – 3505.
[28] Y. A. Abramov, A. Volkov, P. Coppens, *J. Mol. Struct.* **2000**, *529*, 27 – 35.
[29] A. Volkov, PhD thesis, University of New York (Buffalo), **2000**.
[30] A. Bach, D. Lentz, P. Luger, *J. Phys. Chem. A* **2001**, *105*, 7405 – 7412.
[31] D. E. Hibbs, J. Overgaard, R. O. Piltz, *Org. Biomol. Chem.* **2003**, *1*, 1191 – 1198.
[32] E. May, R. Destro, C. Gatti, *J. Am. Chem. Soc.* **2001**, *123*, 12248 – 12254.
[33] J. Overgaard, D. E. Hibbs, *Acta Crystallogr., Sect. A: Found. Crystallogr.* **2004**, 60, 480 – 487.
[34] P. Munshi, T. N. Guru Row, *J. Phys. Chem. A* **2005**, *109*, 659 – 672.
[35] P. Munshi, T. N. Guru Row, *Acta Crystallogr., Sect. B: Struct. Sci.* **2002**, *58*, 1011 – 1017.
[36] P. Munshi, T. N. Guru Row, *Cryst. Growth Des.* **2006**, *6*, 708 – 718.
[37] Y. Zhang, P. Coppens, *Chem. Commun.* **1999**, 2425 – 2426.
[38] N. Bouhmaida, M. Dutheil, N. E. Ghermani, P. Becker, *J. Chem. Phys.* **2002**, *116*, 6196 – 6204.
[39] R. S. Gopalan, G. U. Kulkarni, M. Ravi, C. N. R. Rao, *New J. Chem.* **2001**, *25*, 1108 – 1110.
[40] B. Dittrich, T. Koritsanszky, M. Grosche, W. Scherer, R. Flaig, A. Wagner, H. G. Krane, H. Kessler, C. Riemer, A. M. M. Schreurs, P. Luger, *Acta Crystallogr. Sect. B: Struct. Sci.* **2002**, *58*, 721 – 727.
[41] R. Flaig, T. Koritsanszky, R. Soyka, L. Häming, P. Luger, *Angew. Chem.* **2001**, *113*, 368 – 371; *Angew. Chem. Int. Ed.* **2001**, *40*, 355 – 359; .
[42] P. M. Dominiak, P. Coppens, *Acta Crystallogr., Sect. A: Found. Crystallogr.* **2006**, *62*, 224 – 227.
[43] A. E. Whitten, M. A. Spackman, *Acta Crystallogr., Sect. B: Struct. Sci.* **2006**, *62*, 875 – 888.
[44] E. D. Stevens, P. Coppens, *Acta Crystallogr., Sect. B: Struct. Sci.* **1980**, *36*, 1864 – 1876.
[45] H.-P. Weber, B. M. Craven, *Acta Crystallogr., Sect. B: Struct. Sci.* **1990**, *46*, 532 – 538.
[46] V. Pichon-Pesme, H. Lachekar, M. Souhassou, C. Lecomte, *Acta Crystallogr., Sect. B: Struct. Sci.* **2000**, *56*, 728 – 737.
[47] K. A. Lyssenko, Y. V. Nelyubina, R. G. Kostyanovsky, M. Y. Antipin, *ChemPhysChem* **2006**, *7*, 2453 – 2455.
[48] F. Benabicha, V. Pichon-Pesme, C. Jelsch, C. Lecomte, A. Khmou, *Acta Crystallogr., Sect. B: Struct. Sci.* **2000**, *56*, 155 – 165.
[49] B. Dittrich, PhD thesis, Freie Universität Berlin (Berlin), **2002**.
[50] B. Dittrich, unpublished results.
[51] A. Forni, R. Destro, *Chem. Eur. J.* **2003**, *9*, 5528 – 5537.
[52] R. Boese, N. Niederprüm, D. Bläser, A. Maulitz, M. Y. Antipin, P. R. Mallinson, *J. Phys. Chem. B* **1997**, *101*, 5794 – 5799.
[53] J. W. Bats, P. Coppens, T. F. Koetzle, *Acta Crystallogr., Sect. B: Struct. Sci.* **1977**, *33*, 37 – 45.
[54] P. Coppens, G. Moss, N. K. Hansen, in *Computing in Crystallography* (Eds.: R. Diamond, S. Ramaseshan, K. Venkatesan), Indian Academy of Sciences, Bangalore, **1980**, pp. 16.01 – 16.18.
[55] T. Koritsanszky, J. Buschmann, L. Denner, P. Luger, A. Knochel, M. Haarich, M. Patz, *J. Am. Chem. Soc.* **1991**, *113*, 8388 – 8398.
[56] M. A. Spackman, H.-P. Weber, B. M. Craven, *J. Am. Chem. Soc.* **1988**, *110*, 775 – 782.
[57] S. Swaminathan, B. M. Craven, M. A. Spackman, R. F. Stewart, *Acta Crystallogr., Sect. B: Struct. Sci.* **1984**, *40*, 398 – 404.
[58] H. Birkedal, D. Madsen, R. H. Mathiesen, K. Knudsen, H. P. Weber, P. Pattison, D. Schwarzenbach, *Acta Crystallogr., Sect. A: Found. Crystallogr.* **2004**, *60*, 371 – 381.
[59] F. L. Hirshfeld, H. Hope, *Acta Crystallogr., Sect. B: Struct. Sci.* **1980**, *36*, 406 – 415.
[60] R. Destro, P. Roversi, M. Barzaghi, R. E. Marsh, *J. Phys. Chem. A* **2000**, *104*, 1047 – 1054.
[61] T. W. Hambley, D. E. Hibbs, P. Turner, S. T. Howard, M. B. Hursthouse, *J. Chem. Soc., Perkin Trans. 2* **2002**, 235 – 239.
[62] P. Munshi, T. S. Thakur, T. N. Guru Row, G. R. Desiraju, *Acta Crystallogr., Sect. B: Struct. Sci.* **2006**, *62*, 118 – 127.
[63] D. E. Hibbs, C. J. Austin-Woods, J. A. Platts, J. Overgaard, P. Turner, *Chem. Eur. J.* **2003**, *9*, 1075 – 1084.
[64] S. Swaminathan, B. M. Craven, *Acta Crystallogr., Sect. B: Struct. Sci.* **1984**, *40*, 511 – 518.
[65] B. Fabius, C. Cohen-Addad, F. K. Larsen, M. S. Lehmann, P. Becker, *J. Am. Chem. Soc.* **1989**, *111*, 5728 – 5732.
[66] X. M. He, S. Swaminathan, B. M. Craven, R. K. McMullan, *Acta Crystallogr., Sect. B: Struct. Sci.* **1988**, *44*, 271 – 281.
[67] J. Epstein, J. R. Ruble, B. M. Craven, *Acta Crystallogr., Sect. B: Struct. Sci.* **1982**, *38*, 140 – 149.
[68] R. Destro, R. Bianchi, G. Morosi, *J. Phys. Chem.* **1989**, *93*, 4447 – 4457.
[69] R. Flaig, PhD thesis, Freie Universität Berlin (Berlin), **2000**.
[70] S. Swaminathan, B. M. Craven, R. K. McMullan, *Acta Crystallogr., Sect. B: Struct. Sci.* **1985**, *41*, 113 – 122.
[71] R. Bianchi, G. Gervasio, G. Viscardi, *Acta Crystallogr., Sect. B: Struct. Sci.* **1998**, *54*, 66 – 72.
[72] L. Chen, B. M. Craven, *Acta Crystallogr., Sect. B: Struct. Sci.* **1995**, *51*, 1081 – 1097.
[73] R. Flaig, T. Koritsanszky, D. Zobel, P. Luger, *J. Am. Chem. Soc.* **1998**, *120*, 2227 – 2238.
[74] W. D. Arnold, L. K. Sanders, M. T. McMahon, A. V. Volkov, G. Wu, P. Coppens, S. R. Wilson, N. Godbout, E. Oldfield, *J. Am. Chem. Soc.* **2000**, *122*, 4708 – 4717.
[75] Y. A. Abramov, A. Volkov, G. Wu, P. Coppens, *J. Phys. Chem. B* **2000**, *104*, 2183 – 2188.
[76] B. M. Craven, H.-P. Weber, *Acta Crystallogr., Sect. B: Struct. Sci.* **1983**, *39*, 743 – 748.
[77] H. W. Yang, B. M. Craven, *Acta Crystallogr., Sect. B: Struct. Sci.* **1998**, *54*, 912 – 920.
[78] W. T. Klooster, S. Swaminathan, R. Nanni, B. M. Craven, *Acta Crystallogr., Sect. B: Struct. Sci.* **1992**, *48*, 217 – 227.
[79] T. Koritsanszky, R. Flaig, D. Zobel, H.-G. Krane, W. Morgenroth, P. Luger, *Science* **1998**, *279*, 356 – 358.
[80] F. Hamzaoui, F. Baert, G. Wojcik, *Acta Crystallogr., Sect. B: Struct. Sci.* **1996**, *52*, 159 – 164.
[81] F. Hamzaoui, M. Drissi, A. Chouaih, P. Lagant, G. Vergoten, *Int. J. Mol. Sci.* **2007**, *8*, 103 – 115.
[82] F. Baert, P. Schweiss, G. Heger, M. More, *J. Mol. Struct.* **1988**, *178*, 29 – 48.
[83] F. Hamzaoui, F. Baert, J. Zyss, *J. Mater. Chem.* **1996**, *6*, 1123 – 1130.
[84] B. M. Craven, P. Benci, *Acta Crystallogr., Sect. B: Struct. Sci.* **1981**, *37*, 1584 – 1591.
[85] P. Coppens, Y. Abramov, M. Carducci, B. Korjov, I. Novozhilova, C. Alhambra, M. R. Pressprich, *J. Am. Chem. Soc.* **1999**, *121*, 2585 – 2593.
[86] J. Ellena, A. E. Goeta, J. A. K. Howard, G. Punte, *J. Phys. Chem. A* **2001**, *105*, 8696 – 8708.
[87] J. Ellena, A. E. Goeta, J. A. K. Howard, C. C. Wilson, J. C. Autino, G. Punte, *Acta Crystallogr., Sect. B: Struct. Sci.* **1999**, *55*, 209 – 215.
[88] D. E. Hibbs, J. Overgaard, J. A. Platts, M. P. Waller, M. B. Hursthouse, *J. Phys. Chem. B* **2004**, *108*, 3663 – 3672.
[89] F. Baert, P. Coppens, E. D. Stevens, L. Devos, *Acta Crystallogr., Sect. A: Found. Crystallogr.* **1982**, *38*, 143 – 151.
[90] D. E. Hibbs, S. T. Howard, J. P. Huke, M. P. Waller, *Phys. Chem. Chem. Phys.* **2005**, *7*, 1772 – 1778.
[91] B. M. Craven, R. O. Fox, Jr., H.-P. Weber, *Acta Crystallogr., Sect. B: Struct. Sci.* **1982**, *38*, 1942 – 1952.
[92] R. Guillot, N. Muzet, S. Dahaoui, C. Lecomte, C. Jelsch, *Acta Crystallogr., Sect. B: Struct. Sci.* **2001**, *57*, 567 – 578.
[93] S. T. Howard, M. B. Hursthouse, C. W. Lehmann, E. A. Poyner, *Acta Crystallogr., Sect. B: Struct. Sci.* **1995**, *51*, 328 – 337.
[94] A. Fkyerat, A. Guelzim, F. Baert, W. Paulus, G. Heger, J. Zyss, A. Périgaud, *Acta Crystallogr., Sect. B: Struct. Sci.* **1995**, *51*, 197 – 209.
[95] A. Fkyerat, A. Guelzim, F. Baert, J. Zyss, A. Périgaud, *Phys. Rev. B* **1996**, *53*, 16236 – 16246.
[96] A. Volkov, G. Wu, P. Coppens, *J. Synchrotron Rad.* **1999**, *6*, 1007 – 1015.
[97] L. Lo Presti, R. Soave, R. Destro, *J. Phys. Chem. B* **2006**, *110*, 6405 – 6414.
[98] J. M. Cole, A. E. Goeta, J. A. K. Howard, G. J. McIntyre, *Acta Crystallogr., Sect. B: Struct. Sci.* **2002**, *58*, 690 – 700.

[99] G. K. H. Madsen, F. C. Krebs, B. Lebech, F. K. Larsen, *Chem. Eur. J.* **2000**, *6*, 1797 – 1804.
[100] J. M. Cole, R. C. B. Copley, G. J. McIntyre, J. A. K. Howard, M. Szablewski, G. H. Cross, *Phys. Rev. B* **2002**, *65*, 125107.
[101] X. Li, G. Wu, Y. A. Abramov, A. V. Volkov, P. Coppens, *Proc. Natl. Acad. Sci. USA* **2002**, *99*, 12132 – 12137.

Received: May 15, 2007
Published online on August 6, 2007

